Full-Wave Analysis of Packaged Microwave Circuits with Active and Nonlinear Devices: An FDTD Approach

Chien-Nan Kuo, Bijan Houshmand, *Member, IEEE*, and Tatsuo Itoh, *Fellow, IEEE*

***Abstract*— This paper presents a comprehensive full-wave analysis of packaged nonlinear active microwave circuits by applying the extended finite-difference time-domain (FDTD) method. Based on the approach of using equivalent sources, the device–wave interaction is characterized and incorporated into the FDTD time-marching scheme. As a consequence, analysis of linear and nonlinear properties, including harmonic generation and intermodulation, can be accomplished by employing a large-signal device circuit model. The implementation is first validated by comparing results of FDTD and HP MDS simulation of the circuit without the packaging structure. The analysis then goes beyond the capability of the circuit simulator to include the packaging effect. This analysis is useful in circuit design involving electromagnetic compatibility/electromagnetic interference (EMC/EMI) problems.**

***Index Terms*— EMC/EMI, FDTD, packaging, MESFET, microwave amplifier.**

I. Introduction

THE TREND of microwave circuits has been toward highly integrated systems, such as monolithic microwave integrated circuits (MMIC's), comprising closely spaced elements, discontinuity structures, and passive and active devices. Circuit design in higher frequency range for these complex circuits, especially for nonlinear active circuits in a packaging structure, encounters the severe problem of dealing with the electromagnetic effect of radiation and the coupling effect between different circuit elements. Most commercial design tools for such circuits are based on a circuit approach, in which the *S*-parameter matrix and the harmonic-balance method are applied by dividing the circuit into small elements and cascading the characteristic of each element to obtain the overall system performance. Consequently, the electromagnetic effect is ignored or approximated at best.

Successful circuit design requires the inclusion of the electromagnetic effect. This necessary requirement can be fulfilled by a full-wave approach, which includes the effect by solving Maxwell's equations and taking into account the interaction between electromagnetic waves and circuit elements comprehensively. Since the interaction between electromagnetic waves and active devices affects the system performance significantly, much attention has recently been focused on the incorporation of nonlinear active devices into full-wave analysis. Some frequency-domain techniques utilize the impedance matrix of the devices to achieve this goal. For example, the spectral-domain approach has been extended to analyze hybrid microwave integrated circuits with passive and active lumped elements [1]; the finite-element method (FEM) has been applied to analyze microstrip circuits with a Gunn diode [2].

Among available full-wave techniques, the finite-difference time-domain (FDTD) method attracts researchers' interest most particularly for its direct solution of Maxwell's equations in time domain [3]. Being generally developed, the method has shown its versatility in full-wave modeling of complicated structures, such as planar metallization structures with discontinuities [4] and a leaky-wave antenna with lanchers [5]. It also has wide application to the analysis of picosecond photoconductive switches [6] and interconnects in high-speed digital circuits [7]. Moreover, the conventional algorithm has been extended to the analysis of active microwave circuits, including modal analysis of multiple-oscillator active antennas [9] and small-signal analysis of a MESFET amplifier [10].

Indeed, the advantage of full-wave techniques to go beyond circuit simulators lies in the analysis of microwave circuits involving electromagnetic problems such as electromagnetic compatibility/electromagnetic interference (EMC/EMI). Without sufficient information, circuit design in such problems is accomplished mostly by trial and error. This paper presents the application of the extended FDTD method to the analysis of packaged microwave circuits. A microwave amplifier with a MESFET is used as the platform. Section II begins with a discussion of the modeling of nonlinear active devices. Equivalent voltage/current sources are employed to substitute the devices and, combined with the device circuit model, lead to an equivalent circuit characterizing the device–wave interaction. Section III describes the circuit model of the MESFET. In Section IV, linear and nonlinear properties of the system are examined. Results of FDTD simulation is first compared with those by a HP MDS simulator to validate the implementation, and then the method is applied to the analysis of a packaged amplifier. Finally, conclusions are drawn in Section V.

Manuscript received September 4, 1996; revised December 13, 1996. This work was supportedby Hughes Micro, JSEP under Contract F49620-92-C-0055 and by the U.S. Army Research Office under Contract DAAH04-93-G-0068.

C.-N. Kuo and T. Itoh are with the Electrical Engineering Department, University of California at Los Angeles (UCLA), Los Angeles, CA 90095 USA.

B. Houshmand is with the Jet Propulsion Laboratory, California Institute of Technology, Pasadena, CA 91109 USA.

Publisher Item Identifier S 0018-9480(97)03105-0.

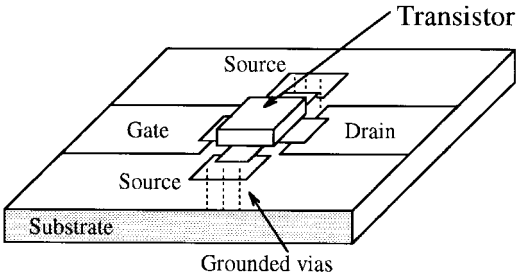

Fig. 1. A packaged transistor connected to the ground plane through vias at the source port in a microstrip circuit.

II. Modeling of Nonlinear Active Devices

Fig. 1 shows a MESFET transistor soldered on the substrate in a microstrip circuit and connected to the ground plane through vias at the source port. This packaged device may occupy several FDTD cells. The modeling of this nonlinear active device needs to carry out the incorporation of the device into the FDTD time-marching algorithm and account for the spatial placement. A possible and complete full-wave method for the modeling can apply a physical model as in [11], which uses a coupled system of Boltzmann's transport equation for carrier transport phenomena and Maxwell's equations for electromagnetic wave propagation. In so doing, difficulty may arise when the physical model is applied to the analysis of a practical microwave circuit. Usually the size of meshes in the device region is required to be much finer than that required in the passive structures of the circuit, which results in the problem of memory limitation or nonuniform meshing.

A feasible method is to represent the device with its lumped circuit model, while the dielectric constant in the device region is enforced to be that of air. Since the size of a device is typically much smaller than a wavelength, this method produces reasonable approximation and still retains a high degree of accuracy in full-wave analysis. Even in the case where the size of a device is comparable to a wavelength (e.g., some power devices with large gate width), the method can also be applied by cutting the device region into several slices, each represented by a lumped circuit model. Although the dimension of a lumped circuit is zero, the effect from the spatial distribution and the packaging structure has already been considered by adding parasitic elements, inductors, and capacitors in the circuit model to account for the time delay as waves propagate through the device.

Hence, the key concept of the incorporation is to connect quantities of electromagnetic fields with quantities of the circuit model. Direct implementation places the lumped circuit in the device region and matches internal nodes of the lumped circuit with FDTD grids as used in [7]–[9]. Each circuit element, placed on the edge of a FDTD cell as a two-terminal element, can be directly incorporated into the FDTD algorithm as the formulation in [12], [13]. Alternative implementation is to place effective electric currents, or equivalently, current sources [14], in the device region. Differently derived, a dual approach utilizes effective magnetic currents, or voltage sources [15]. This implementation of using equivalent sources is more general than the direct implementation in the sense

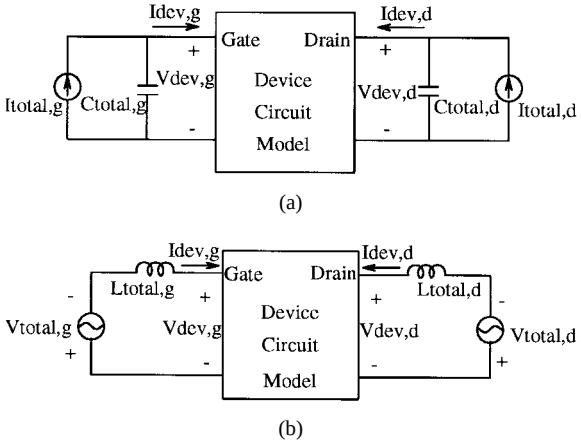

Fig. 2. (a) The Norton-equivalent circuit governing the device–wave interaction. (b) The Thevenin-equivalent circuit.

of formulation for complex circuit models and more advantageous for the modeling of a multiport device. These equivalent sources characterize not only the scattering properties but also the voltage–current relationship at each port. One end of each equivalent source connects to the microstrip line and the other to a grounded via, which provides a voltage reference as well as the modeling of the vias at the source port. It is suggested that a number of equivalent sources should be placed across the whole width of the microstrip line in order to avoid additional current discontinuity at the junction [16]. Physically speaking, these equivalent current and voltage sources stand for the device current and voltage at each port, respectively.

Connecting field quantities and circuit quantities, the equivalent sources serve as dependent sources, the values of which satisfy both Maxwell's equations and the device circuit model. Because voltage and current relate to the integration of the *E*- and *H*-field, respectively, the governing equation for field updating is derived by taking integration of Maxwell's equations over those FDTD cells containing the equivalent sources. The integral form of Ampere's equation at each port yields to

$$C_{\text{total}}\frac{dV_{\text{dev}}}{dt} + I_{\text{dev}} = I_{\text{total}}. \tag{1}$$

Together with the device circuit model, this equation leads to an equivalent circuit characterizing the device–wave interaction as shown in Fig. 2(a). The pair of a current source and a shunt capacitor denotes the Norton-equivalent circuit of FDTD cells as seen by the device. Similarly, the integral form of Faraday's equation yields to

$$-L_{\text{total}}\frac{dI_{\text{dev}}}{dt} - V_{\text{dev}} = V_{\text{total}} \tag{2}$$

and the equivalent circuit is shown in Fig 2(b), where the Thevenin-equivalent circuit of FDTD cells consists of a voltage source and a series inductor. The capacitance C_{total} means the total space capacitance of FDTD cells at each port, while the inductance L_{total} is the total space inductance.

In each time advance, the device voltage is evaluated from the state equation of the circuit in Fig. 2 and subsequently used to update the electromagnetic fields in the equivalent-source region. The state equation can be generally expressed

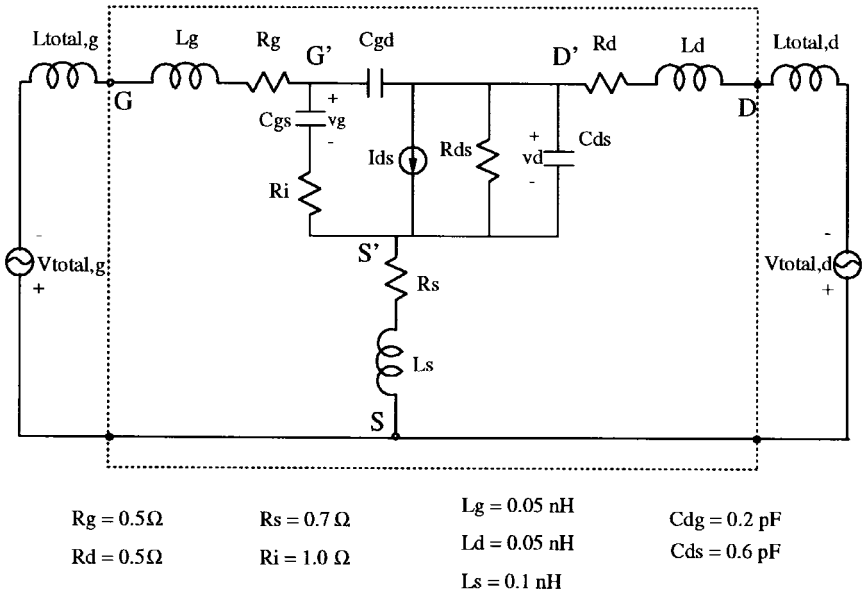

Fig. 3. Inside the dashed box is the large-signal device circuit model of a MESFET used in this paper. The gate-source capacitor $C_{\rm gs}$ and the drain current source $I_{\rm ds}$ are nonlinear.

as a nonlinear differential equation by

$$\mathbf{A}(\mathbf{X})\cdot\frac{d\mathbf{X}}{dt}=\mathbf{B}(\mathbf{X})\cdot\mathbf{X}+\mathbf{F}(\mathbf{X}) \tag{3}$$

where the vector $\mathbf{X}$ denotes the state variables, the matrices $\mathbf{A}$ and $\mathbf{B}$ are derived from the circuit elements, and the forcing term $\mathbf{F}$ comes from the source, $I_{\rm total}$ or $V_{\rm total}$. Performing the forward difference scheme yields to a finite difference equation by

$$\begin{aligned}\mathbf{G}(\mathbf{X}_{n+1})\equiv&\frac{\mathbf{A}(\mathbf{X}_{n+1})}{\Delta t}\cdot(\mathbf{X}_{n+1}-\mathbf{X}_n)\\&-\mathbf{B}(\mathbf{X}_{n+1})\cdot\mathbf{X}_{n+1}-\mathbf{F}(\mathbf{X}_{n+1})=0\end{aligned} \tag{4}$$

where the subscript denotes the time step. Afterwards, iterative searching for $\mathbf{X_{n+1}}$ is performed by the Newton–Raphson method [17], a multidimensional root finding method. Given $\mathbf{X}_n$ as the initial value, $\mathbf{X}_{n+1}$ is calculated iteratively until it converges by

$$\mathbf{X}_{n+1}^{j+1}=\mathbf{X}_{n+1}^{j}-[\mathbf{J}(\mathbf{X}_{n+1})]^{-1}\big|^{j}\cdot\mathbf{G}(\mathbf{X}_{n+1}^{j}) \tag{5}$$

where $\mathbf{J}$ is the Jacobian matrix and its elements are defined as

$$J_{pq}\equiv\frac{\partial G_p}{\partial x_q}. \tag{6}$$

The criterion of numerical stability is not only to satisfy the Courant condition in the FDTD algorithm but also to choose Δt such that $\mathbf{J}$ is not singular. Typically the Δt chosen for the former criterion is the order of pico seconds for microwave circuits, much smaller than that for the latter as the order of nano-second, so it causes no numerical burden because of choosing a smaller Δt.

III. Device Circuit Model

In this paper, the large-signal circuit model of a MESFET in FDTD simulation is illustrated inside the dashed box in Fig. 3, which also includes the Thevenin-equivalent circuit of FDTD cells. The internal nodes *G*', *D*', *S*' represent the intrinsic part of the MESFET. This circuit model contains two nonlinear elements, the gate–source capacitor $C_{\rm gs}$ and the drain current $I_{\rm ds}$. Governed by the *PN*-junction capacitance model, the gate–source capacitor is expressed as

$$C_{\rm gs}(v_g)=\frac{C_{gso}}{\sqrt{1-v_g/\phi_{bi}}}. \tag{7}$$

The drain current $I_{\rm ds}$, describing dc characteristics, relates to v_g and v_d as

$$I_{\rm ds}(v_g,v_d)=(A_0+A_1v_{G'S'}+A_2v_{G'S'}^2+A_3v_{G'S'}^3)\tanh(\alpha v_d). \tag{8}$$

Those parameters are listed in Table I. The dc characteristic is plotted in Fig. 4.

After choosing state variables as $[\,v_g,v_{G'D'},v_d,i_{L_g},i_{L_d}]^T$, it is straightforward to derive the state equation from the nodal equation of the circuit. The resultant matrices in the state

$$\mathbf{A}=\begin{bmatrix}C_{\rm gs}(v_g)&0&0&0&0\\C_{\rm gs}(v_g)&C_{\rm gd}&0&0&0\\0&C_{\rm gd}&-C_{\rm ds}&0&0\\0&0&0&G_g[(\frac{G_g}{G}-1)L_g'-\frac{G_s}{G}L_s]&G_g[\frac{G_d}{G}L_d'-\frac{G_s}{G}L_s]\\0&0&0&G_d[\frac{G_g}{G}L_g'-\frac{G_s}{G}L_s]&G_d[(\frac{G_d}{G}-1)L_d'-\frac{G_s}{G}L_s]\end{bmatrix} \tag{9}$$

TABLE I
PARAMETERS FOR NONLINEAR ELEMENTS IN THE CIRCUIT MODEL

C_{gso}	ϕ_{bi}	A_0	A_1	A_2	A_3	α
3pF	0.7V	0.5304	0.2595	-0.0542	-0.0305	1.0

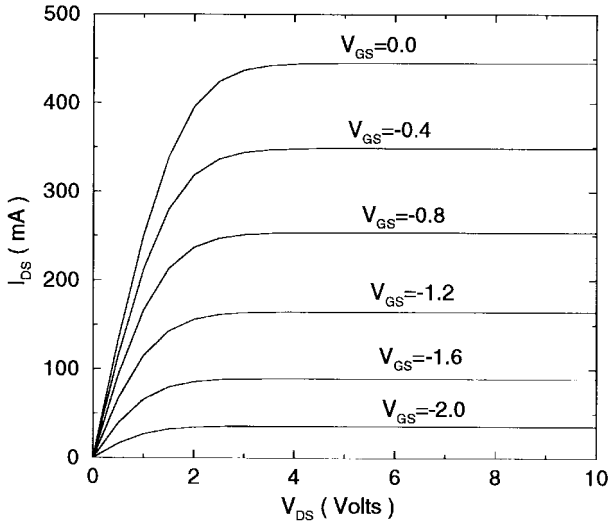

Fig. 4. DC characteristics of the MESFET.

equation are found as (see (9) at the bottom of the previous page)

$$\mathbf{B}=\begin{bmatrix} -G_{\rm gs} & G_{\rm gs} & G_{\rm gs} & 0 & 0 \\ 0 & 0 & 0 & 1 & 0 \\ 0 & 0 & 0 & 0 & -1 \\ 0 & G_g(1-\frac{G_g}{G}) & G_g\frac{G_s}{G} & 1 & 0 \\ 0 & -G_d\frac{G_g}{G} & G_d\frac{G_s}{G} & 0 & 1 \end{bmatrix} \tag{10}$$

$$\mathbf{F}=\begin{bmatrix} 0 \\ 0 \\ I_{\rm ds}(v_g,v_d) \\ G_g(1-\frac{G_g}{G})V_{{\rm total},g}-G_g\frac{G_d}{G}V_{{\rm total},d} \\ -G_d\frac{G_g}{G}V_{{\rm total},g}+G_d(1-\frac{G_d}{G})V_{{\rm total},d} \end{bmatrix} \tag{11}$$

where some notations are defined as

$$L_g^{'}\equiv L_g+L_{{\rm total},g}$$
$$L_d^{'}\equiv L_d+L_{{\rm total},d}$$
$$G=G_g+G_d+G_s$$
$$\text{and}\quad G_g=1/R_g;\quad G_d=1/R_d;\quad G_s=1/R_s.$$

Note that $\mathbf{B}$ is independent of the state variables. The iterative formula for $\mathbf{X}_{n+1}$ is

$$\mathbf{X}_{n+1}^{j+1}=\mathbf{X}_{n+1}^{j}-\{\frac{1}{\Delta t}(\frac{\partial \mathbf{A}}{\partial v_g}+\mathbf{A})-\mathbf{B}-\frac{\partial \mathbf{F}}{\partial \mathbf{X}_{n+1}}\}^{-1}\mathbf{f}(\mathbf{X}_{n+1}^{j}). \tag{12}$$

The device voltage is evaluated by

$$V_{{\rm dev},i}=-V_{{\rm total},i}-L_{{\rm total},i}\frac{di_{L_g}}{dt} \tag{13}$$

where i means the gate or the drain port.

IV. SIMULATION

The system under consideration is a microwave amplifier containing a MESFET as shown in Fig. 5. A perfectly electronic conductor (PEC) box is used for the modeling of a packaging structure. There are two rectangular holes at the input/output ports for feeding power. The circuit model of the MESFET is described in Section III. The amplifier excludes biasing circuits, so dc biasing is established by directly applying dc sources, V_{gg} and V_{dd}, each with a source impedance of 50 Ω, at the input/output ports. The biasing conditions chosen are $V_{\rm GS}=-0.81$ V and $V_{\rm DS}=6.4$ V. The circuit is designed to match at 6 GHz. The size of the MESFET, which resides in the region of 80 mil in the longitudinal direction, is much smaller than the guided wavelength at 6 GHz.

The extended FDTD method of using the equivalent voltage-source approach is applied to obtain time responses. The computation domain is divided into uniform meshes of dimensions 74 $\times$ 40 $\times$ 128. The space steps chosen are $\Delta_x=10$ mil, $\Delta_y=7.75$ mil, and $\Delta_z=10$ mil. Higdon's second-order absorbing boundary condition (ABC) [18] is applied on the truncated boundary to absorb out-going waves. The metal is assumed to be a perfect conductor of zero thickness. There are ten and eight equivalent voltage-sources employed to replace the transistor at the gate and drain ports, respectively. FDTD simulation starts with dc excitation by using an exponential rising function to reduce the transient time, and then an ac signal is imposed upon the input port. The formulation of incorporating a dc source with a source impedance into the FDTD algorithm is depicted in [12].

A. Analysis of the Circuit Without the Packaging Structure

The method is first applied to examine the small-signal response of the circuit without the packaging box. In paper [10], results of FDTD simulation applying a small-signal device model have been validated by comparison with measured data in good agreement. Different from [10], this paper applies the nonlinear large-signal model. A Gaussian pulse modulated at 6 GHz is used as the ac signal and the amplitude is small to allow the circuit to operate in the linear region. The incident wave is the measured voltage in the system of a semi-infinite microstrip line. Ac responses are obtained by subtracting the time responses to those of pre-simulated dc-only excitation. The *S*-parameters are calculated from the reflected and transmitted waves.

A circuit simulator, HP MDS, is also applied to simulate the circuit. Particularly, the vias at the source port are considered by adding an inductor of 0.05 nH, a typical inductance, connecting the source port to the ground nodes. According to the device model used in FDTD simulation, suitable parameters are set to choose the Curtice cubic model for the drain current as well as the capacitance model and the junction current model. Both results of FDTD and HP MDS simulation are plotted in Fig. 6 for comparisons. The matching dip of FDTD simulation is at 5.58 GHz, deviating from that of HP MDS simulation for 7% in this case. This deviation may come from the modeling of the vias at the source port. The frequency of

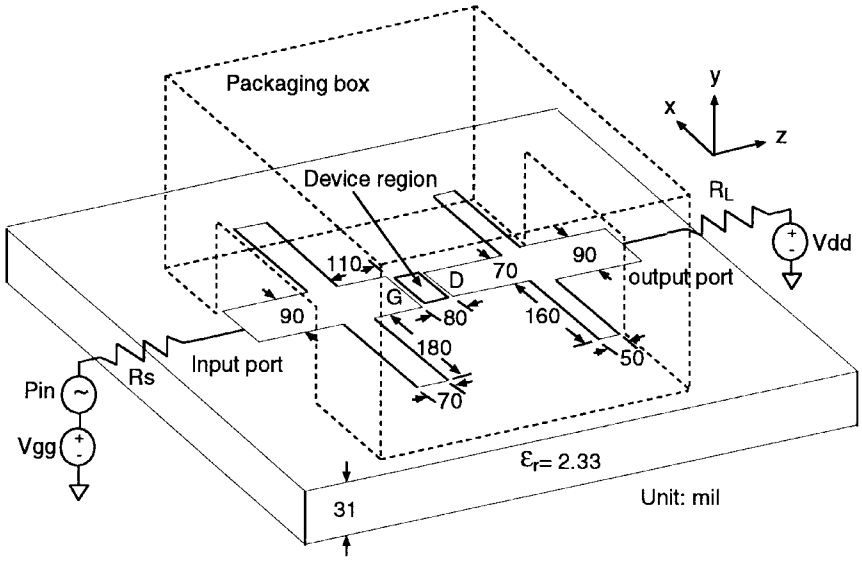

Fig. 5. The structure and the dimension of a microwave amplifier. The packaging structure is modeled as a PEC box with two holes at the input/output ports for feeding power.

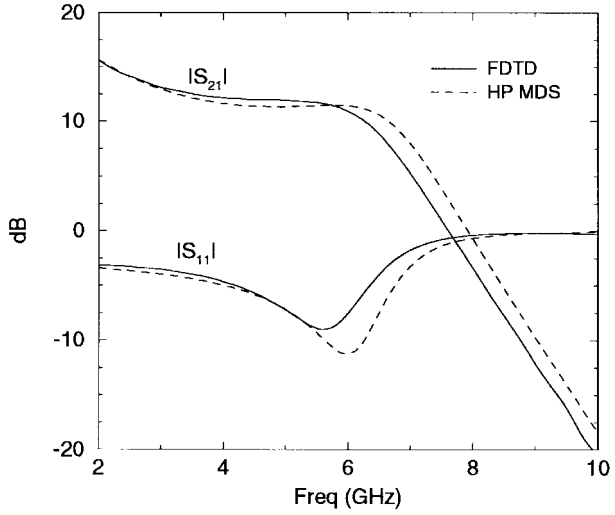

Fig. 6. Small-signal analysis of the microwave amplifier, without the packaging box, applying the large-signal circuit model.

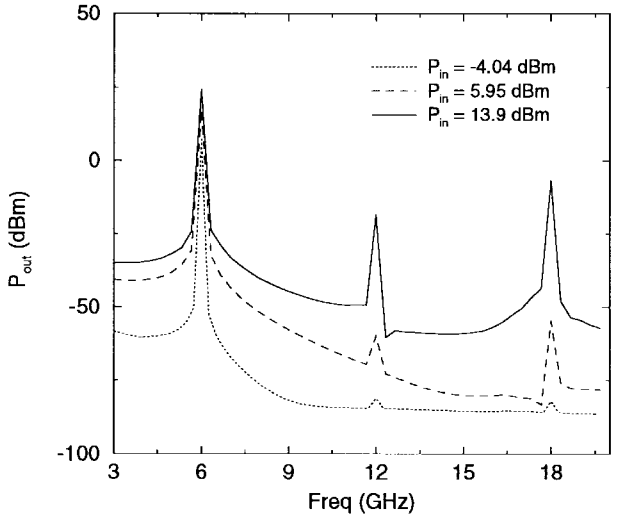

Fig. 7. The spectrum of the output power using single-tone excitation of different power levels at 6 GHz.

the matching dip is sensitive to the effective inductance of the vias, which cause series feedback effect. It is found that in HP MDS simulation, the frequency of the matching dip decreases as the inductance decreases.

Nonlinear phenomena is also inspected by evaluating the output power, which is the dissipated power calculated from the voltage across the loading resistor R_L by the definition of

$$P_{\text{out}}(\omega) = \frac{V_L(\omega)^2}{R_L} \tag{14}$$

where frequency-domain information is obtained by taking Fourier transform on the steady-state response. Single-tone excitation produces output power at harmonics due to the nonlinearity. Fig. 7 illustrates the spectrum of the output power with different levels of the input power at 6 GHz. Note that the output power appears at harmonic frequencies only. The power between harmonics is actually the numerical noise from the Fourier transform. Applying larger time sequences can lower the numerical noise. In HP MDS simulation, the output power is stem lines at harmonic frequencies. This is clear when comparing both results in Fig. 8, which show the curves of the output power to the input power for different harmonics. The power at the 1-dB compression point is 25.1 dB. In this simulation, it takes 15 000 time steps for each input power level, and the execution time takes about 6.5 h using the SUN Ultra 1 Model 140 workstation.

Intermodulation is inspected by two-tone excitation at 3 and 6 GHz of the same input power level. The spectrum of the output power for different input power levels is plotted in Fig. 9. The output power appears only at the frequency of mixing frequencies, or intermodulation products, which arise as linear combinations of 3 and 6 GHz. For low input power, the numerical noise in this analysis might be too large to obtain accurate output power. The output power of different

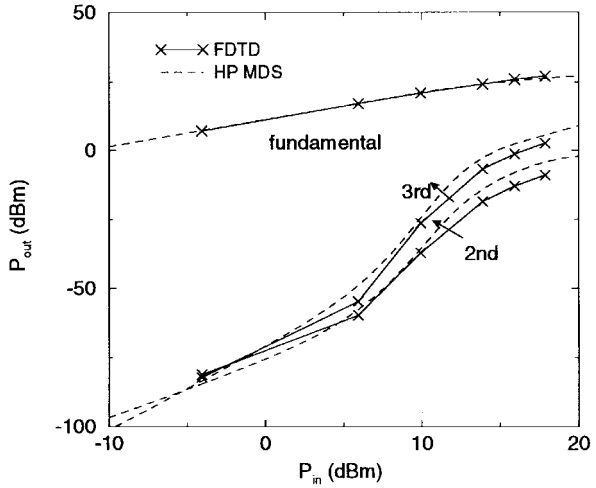

Fig. 8. The output power of harmonics using single-tone excitation.

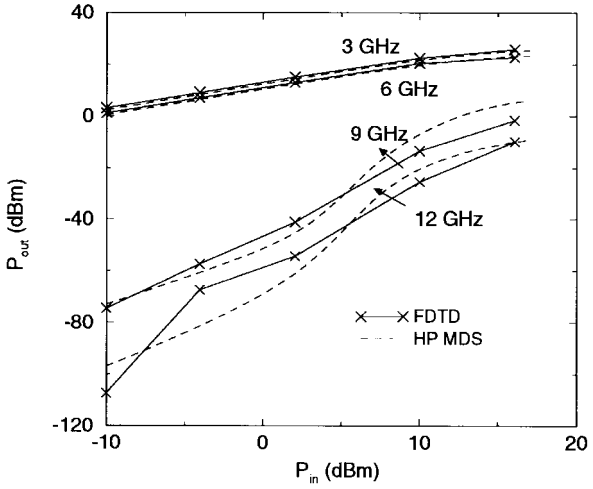

Fig. 10. The output power of intermodulation products using two-tone excitation.

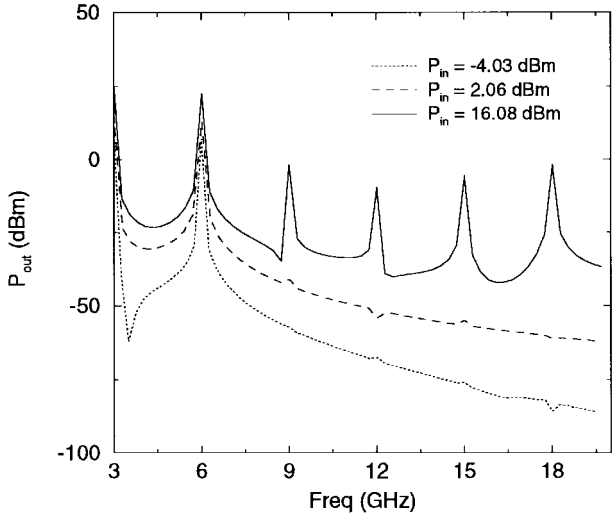

Fig. 9. The spectrum of the output power using two tones of the same power level $P_{\rm in}$ at 3 and 6 GHz.

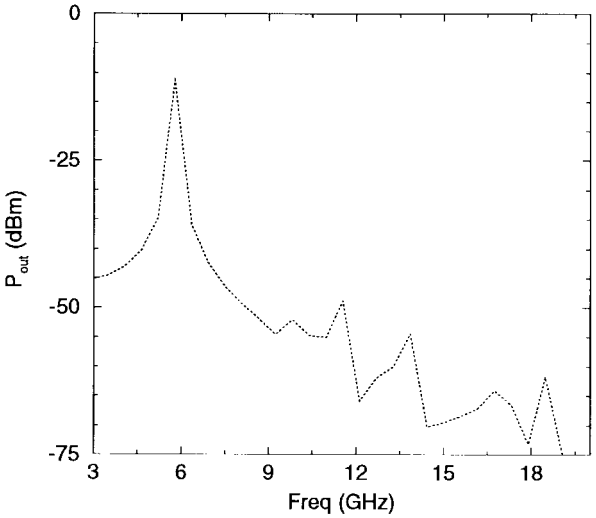

Fig. 11. The spectrum of the output power in the case that a small-signal Gaussian pulse modulated at 6 GHz is imposed upon a packaged amplifier, an example showing the circuit oscillating after being placed in a packaging structure.

intermodulation products is shown in Fig. 10. These results of nonlinear analysis by FDTD simulation are in good agreement with those obtained by HP MDS simulation. The analysis of these system responses verifies the capability of the extended FDTD method in dealing with nonlinear active microwave circuits.

B. Analysis of the Circuit with the Packaging Structure

When the circuit is placed in a packaging structure, an interesting question arises—how does the packaging structure affects circuit performance? The analysis of a packaged circuit is beyond the capability of circuit simulators but can be accomplished by the extended FDTD method by including the circuit as well as the packaging structure in the analysis as a whole. Physically, the packaging structure forms a partially dielectric-filled cavity. Excited by the circuit, the cavity stores energy due to the natural resonance and the stored energy is inevitably coupled back to the circuit. To a nonlinear active circuit, this feedback makes the stability circles drift and may result in oscillation. An example is the analysis of the circuit with a packaging box of dimensions 1560 mil $\times$ 186 mil $\times$ 1250 mil. The first resonant frequency of this packaging structure is found at 5.72 GHz by FDTD pre-simulation of a packaged uniform microstrip line. Using a small-signal Gaussian pulse modulated at 6 GHz, close to the resonant frequency, the output power indicates that the packaging structure interacts with the circuit heavily and the circuit is oscillating at the resonant frequency as shown in Fig. 11.

In order to avoid oscillation, dimensions of the packaging structure are usually chosen such that the resonant frequency is raised far above the frequency range of interest. For this purpose, the dimensions of the packaging box are changed to be 640 mil $\times$ 186 mil $\times$ 690 mil. The first resonant frequency moves higher at 11.79 GHz. The packaged circuit therefore becomes stable. Fig. 12 shows the effect of the packaging

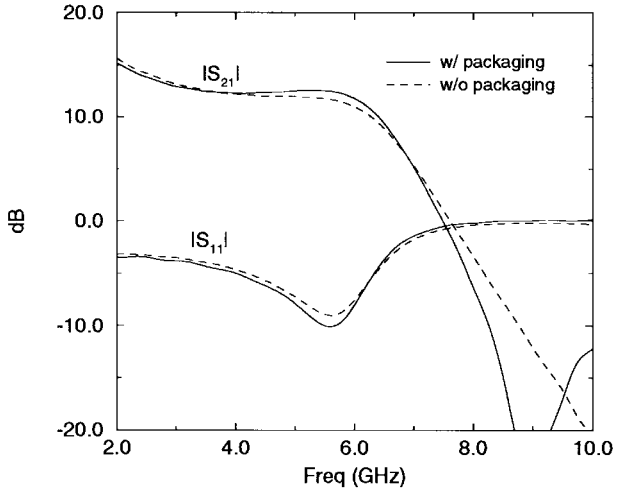

Fig. 12. Investigation of the packaging effect on the small-signal analysis by excitation of a modulated Gaussian pulse.

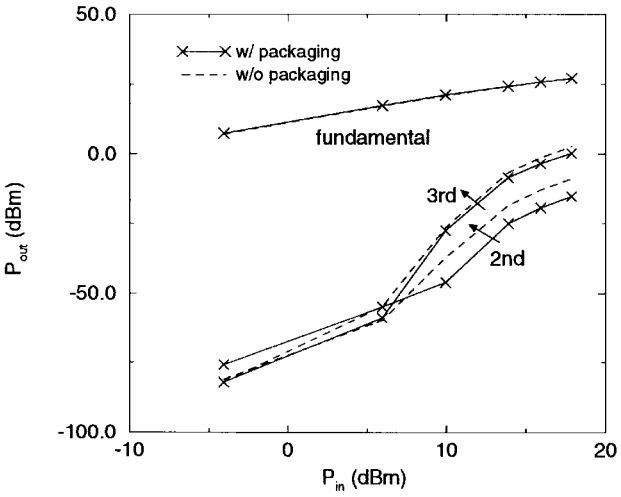

Fig. 13. The packaging effect on the large-signal analysis by a single-tone excitation at 6 GHz.

structure on *S*-parameters. In this case, the frequency of the matching dip remains the same at 5.58 GHz but the magnitude changes from -8.98 to -10.07 dB, while the gain at 6 GHz varies from 10.95 to 11.76 dB. The packaging effect on the output power of a single-tone excitation at 6 GHz is shown in Fig. 13. The resonant frequency is close to that of the second harmonic, so energy is coupled to the second harmonic strongly and its power curve varies more significantly than others.

V. Conclusion

This paper employs the extended FDTD method to comprehensive simulation of a packaged microwave amplifier, which includes a nonlinear active three-terminal device. Being substituted by equivalent voltage sources in the device region, the device can be represented by its lumped large-signal circuit model with the spatial effect considered. An equivalent circuit is accordingly derived to characterize the device–wave interaction. An iterative scheme is applied to evaluate the device voltage and update the electromagnetic fields in the device region. Based on this approach, linear and nonlinear properties of the circuit without the packaging structure are analyzed and results are in good agreement with those of HP MDS simulation. The approach is also performed to investigate the packaging effect, a cavity effect affecting stability circles and resulting in oscillation in certain case.

In general, full-wave analysis is applicable to packaged nonlinear active circuits in case the device circuit model is available, even in very high frequency. Although full-wave simulators are still much more time-consuming as compared to circuit simulators, this analysis becomes necessary and provides useful information for circuit design in the environment where electromagnetic effect of radiation and coupling effect must be considered.

References

[1] T.-S. Horng, "Extending the three-dimensional spectral-domain approach to hybrid microwave integrated circuits with passive and active lumped elements," in *1994 IEEE MTT-S Int. Microwave Symp. Dig.*, San Diego, CA, May 1994, pp. 709–712.

[2] K. Guillouard, M. F. Wong, V. F. Hanna and J. Citerne, "A new global finite element analysis of microwave circuits including lumped elements," in *1996 IEEE MTT-S Int. Microwave Symp. Dig.*, San Francisco, CA, June 1996, pp. 355–358.

[3] A. Taflove, *Computational Electrodynamics: The Finite-Difference Time-Domain Method.* Norwood, MA: Artech House, 1995, ch. 1.

[4] D. M. Sheen, S. M. Ali, M. D. Abouzahra, and J. A. Kong, "Application of the three-dimensional finite-difference time-domain method to the analysis of planar microstrip circuits," *IEEE Trans. Microwave Theory Tech.*, vol. 38, pp. 849–857, July 1990.

[5] M. Chen, H. Z. Chang, B. Houshmand, and T. Itoh, "Characterization of leaky wave antenna and active gain enhancement," in *Proc. 26th EUMC*, Prague, Czech., Sept. 1996, pp. 579–582.

[6] E. Sano and T. Shibata, "Fullwave analysis of picosecond photoconductive switches," *IEEE J. Quantum Electron.*, vol. 26, pp. 372–377, Feb. 1990.

[7] M. Piket-May, A. Taflove, and J. Baron, "FD-TD modeling of digital signal propagation in 3-D circuits with passive and active loads," *IEEE Trans. Microwave Theory Tech.*, vol. 42, pp. 1514–1523, Aug. 1994.

[8] Y.-S. Tsuei, A. C. Cangellaris, and J. L. Prince, "Rigorous electromagnetic modeling of chip-to-package (first-level) internonnections," *IEEE Trans. Comp., Hybrids, Manufact. Technol.*, vol. 16, pp. 876–883, Dec. 1993.

[9] B. Toland, J. Lin, B. Houshmand, and T. Itoh, "FDTD analysis of an active antenna," *IEEE Microwave Guided Wave Lett.*, vol. 3, pp. 423–425, Nov. 1993.

[10] C.-N. Kuo, V. A. Thomas, S. T. Chew, B. Houshmand, and T. Itoh, "Small signal analysis of active circuits using FDTD algorithm," *IEEE Microwave Guided Wave Lett.*, vol. 5, pp. 216–218, July 1995.

[11] M. A. Alsunaidi, S. M. Sohel Imtiaz, and S. M. El-Ghazaly, "Electromagnetic wave effects on microwave transistors using a full-wave time-domain model," *IEEE Trans. Microwave Theory Tech.*, vol. 44, pp. 799–808, June 1996.

[12] W. Sui, D. A. Christensen and C. H. Durney, "Extending the two-dimensional FD-TD method to hybrid electromagnetic systems with active and passive lumped elements," *IEEE Trans. Microwave Theory Tech.*, vol. 40, pp. 724–730, Apr. 1992.

[13] B. Toland, B. Houshmand, and T. Itoh, "Modeling of nonlinear active regions with the FDTD method," *IEEE Microwave Guided Wave Lett.*, vol. 3, pp. 333–335, Sep. 1993.

[14] V. A. Thomas, M. E. Jones, M. Piket-May, A. Taflove, and E. Harrigan, "The use of SPICE lumped circuits as sub-grid models for FDTD analysis," *IEEE Microwave Guided Wave Lett.*, vol. 4, pp. 141–143, May 1994.

[15] C.-N. Kuo, R.-B. Wu, B. Houshmand, and T. Itoh, "Modeling of microwave active devices using the FDTD analysis based on the voltage-source approach," *IEEE Microwave Guided Wave Lett.*, vol. 6, pp. 199–201, May 1996.

[16] C.-N. Kuo, B. Houshmand, and T. Itoh, "FDTD analysis of active circuits with equivalent current source approach," in *1995 IEEE AP-S Int. Symp. Dig.*, Newport Beach, CA, June 1995, pp. 1510–1513.

[17] J. Choma, *Electrical Networks: Theory and Analysis.* New York: Wiley, 1985. ch. 6.
[18] R. L. Higdon, "Absorbing boundary conditions for difference approximations to the multi-dimensional wave equation," *Math. Comput.,* vol. 47, no. 176, pp. 437–459, Oct. 1986.

Chien-Nan Kuo received the B. S. degree in electronic engineering from National Chiao-Tung University, Hsin Chu, Taiwan, and the M. S. degree in electrical engineering from National Taiwan University, Taipei, Taiwan, in 1988 and 1990, respectively. He is currently pursuing the Ph.D. degree at the University of California, Los Angeles (UCLA).

From 1992 to 1993, he worked as a Research Assistant at the Institute of Information Science, Academic Sinica, Nankang, Taiwan. Since 1993, he has been a Graduate Student Researcher in the Department of Electrical Engineering, UCLA. His research interests include the characterization of microwave and millimeter-wave integrated circuits, the simulation for the electric performance of electronic packaging, and the development of electromagnetic simulation tools.

Bijan Houshmand (S'86–M'90) received the B.S., the M.S. and the Ph.D. degrees in electrical and computer engineering from the University of Illinois, Urbana, in 1984, 1985, and 1990, repsectively.

He has been a Visiting Assistant Professor at the University of Illinois and the University of California, Los Angeles (UCLA), where he taught and conducted research in numerical electromagnetics with applications to scattering, radiation, and propagation problems. He is currently a member of the technical staff at the Jet Propulsion Laboratory, California Institute of Technology, Pasadena, CA.

Dr. Houshmand is a member of Tau Beta Pi and URSI Commission B.

Tatsuo Itoh (S'69–M'69–SM'74–F'82) received the B.S. and M.S. degrees from Yokohama National University, Japan, in 1964 and 1968, repsectively, and the Ph. D. degree in electrical engineering from the University of Illinois, Urbana, in 1969.

From September 1966 to April 1976, he was with the Electrical Engineering Department, University of Illinois. From April 1976 to August 1977, he was a Senior Research Engineer at the Radio Physics Laboratory, SRI International, Menlo Park, CA. From August 1977 to June 1978, he was an Associate Professor at the University of Kentucky, Lexington. In July 1978, he joined the faculty at the University of Texas at Austin, where he became a Professor of electrical engineering in 1981 and Director of the Electrical Engineering Research Laboratory in 1984. During the summer of 1979, he was a Guest Researcher at AEG-Telefunken, Ulm, West Germany. In September 1983, he was selected to hold the Hayden Head Centennial Professorship of Engineering at the University of Texas. In September 1984, he was appointed Associate Chairman for Research and Planning of the Electrical and Computer Engineering Department, the University of Texas. In January 1991, he joined the University of California, Los Angeles (UCLA), as Professor of electrical engineering and Holder of the TRW Endowed Chair in microwave and millimeter-wave electronics. He is currently Director of Joint Services Electronics Program (JSEP) and is also Director of Multidisciplinary University Research Initiative (MURI) program at UCLA. He was an Honorary Visiting Professor at Nanjin Institute of Technology, China, and Japan Defense Academy. In April 1994, he was appointed an Adjunct Research Officer for Communications Research Laboratory, Ministry of Post and Telecommunication, Japan. He currently holds a Visiting Professorship at the University of Leeds, U.K., and is an External Examiner of the graduate program, City University of Hong Kong.

Dr. Itoh is a member of the Institute of Electronics and Communication Engineers of Japan, and Commissions B and D of USNC/URSI. He served as the Editor of IEEE TRANSACTIONS ON MICROWAVE THEORY AND TECHNIQUES from 1983 through 1985. He serves on the Administrative Committee of IEEE Microwave Theory and Techniques Society. He was Vice President of the Microwave Theory and Techniques Society in 1989 and President in 1990. He was the Editor-in-Chief of IEEE MICROWAVE AND GUIDED WAVE LETTERS from 1991 through 1994. He was the Chairman of USNC/URSI Commission D from 1988 to 1990, Vice Chairman of Commission D of the International URSI for 1991–1993 and Chairman of the same Commission. for 1993–1996. He is on the Long Range Planning Committee of URSI. He serves on advisory boards and committees of a number of organizations including the National Research Council and the Institute of Mobile and Satellite Communication, Germany.